

# Correlation between ir Spectra, X-Ray Diffraction, and Distribution of Structural Vacancies in $\text{Fe}^{3+}[\square_{\delta}\text{Fe}_{1-3\delta}^{2+}\text{Fe}_{(1-x)+2\delta}\text{M}_x^{3+}]\text{O}_4^{2-}$ -Type Spinel

B. GILLOT AND F. BOUTON

*Laboratoire de Recherches sur la Réactivité des Solides associé au CNRS, Faculté des Sciences Mirande, B.P. 138, 21004 Dijon Cedex, France*

Received January 17, 1979; in revised form July 18, 1979

The effect of particle size, substitution, and conversion ratio on the formation of vacancy-ordered superstructure in spinels of  $\text{Fe}^{3+}[\square_{\delta}\text{Fe}_{1-3\delta}^{2+}\text{Fe}_{(1-x)+2\delta}\text{M}_x^{3+}]\text{O}_4^{2-}$  type has been investigated using X-ray diffraction and ir spectrometry. For substitution ratios  $x = 0.27$ , the existence—from a given conversion ratio ( $\alpha > 0.76$ )—of superstructure rays and of a large number of absorption bands confirms a vacancy and cation ordering on octahedral sites. For substitution ratios  $x > 0.40$  no vacancy ordering could be detected. It has also been shown that vacancies are only partially ordered for fully oxidized magnetite samples whose crystallite size is 100 Å.

## Introduction

There are still numerous studies about the distribution and ordering of vacancies in the iron sesquioxide  $\gamma\text{-Fe}_2\text{O}_3$  (1-3). It is generally agreed that  $\gamma\text{-Fe}_2\text{O}_3$  resulting from the oxidation of finely divided magnetite, at low temperature, has a spinel structure with ordered vacancies on octahedral sites (sites B); however, several exceptions have been reported. They suggest either the possible nonordering of vacancies on octahedral sites although these vacancies are all in those sites or the distribution of those vacancies on both octahedral and tetrahedral sites (sites A).

In the former case, only  $\gamma\text{-Fe}_2\text{O}_3$  particles of size smaller than about 200 Å show a disordered distribution (2). Takei and Chiba (4) have also found a disordered distribution of vacancies on B sites with films of  $\gamma\text{-Fe}_2\text{O}_3$  epitaxially grown on a (100) surface of MgO by the halide-decomposition method.

In the latter case, the simultaneous distribution of vacancies on both types of sites

has been mainly observed for  $\gamma\text{-Fe}_2\text{O}_3$  samples prepared differently from the former, i.e., by dehydrating  $\gamma\text{-FeOOH}$  around 200°C or by oxidizing  $\text{Fe}_3\text{O}_4$  which is obtained by treating equal volumes of a mixture of  $\text{FeCl}_3$  and  $\text{FeCl}_2$  with NaOH at 40°C. Korobeinikova *et al.* (1), referring to the values of the intensity ratio of the (440) and (400) X-ray reflections with various theoretical distributions of vacancies in the cationic sublattice, determined the vacancy concentration on the tetrahedral and octahedral sites of the spinel structure of iron oxide specimens obtained by different methods.

In previous papers (5, 6) using X-ray and ir spectrometry, we showed that the oxidation of finely divided aluminum- or chromium-substituted magnetites also resulted in lacunar spinels of  $(\text{Fe}_{8-8y}\text{M}_{8y}^{3+}\square)\text{O}_{12}^{2-}$  type, which exhibited a vacancy ordering on octahedral sites for low substitution ratios ( $y < 0.26$ ). Being also interested in the influence of crystallite size

on the oxidation kinetics of magnetite as well as the  $\gamma$ -phase conversion, thus obtained, into  $\alpha$  rhombohedral phases when that size approaches 4000 Å, we showed superstructure rays for partially oxidized magnetites. As they can be structurally formulated as  $\text{Fe}^{3+}[\text{Fe}_{1+2\delta}^{3+}\text{Fe}_{1-3\delta}^{2+}\square_{\delta}]_2\text{O}_4^{2-}$  ( $0 < \delta < 1/3$ ) and be considered as homogeneous, mixed phases, they show a vacancy and cation ordering on octahedral sites for a vacancy ratio less than 1/3.

Following partial results obtained by X-ray analysis and ir spectrometry the present paper shows more clearly (using both techniques which proved supplements) the influence of the conversion ratio and crystallite size of pure and slightly substituted magnetites upon vacancy ordering.

### Samples

The preparation and characterization conditions (X ray, TDA, electron microscopy, chemical analysis, specific area) of pure magnetite samples of various sizes or of aluminum- or chromium-substituted magnetites have already been reported (5, 6). In particular, magnetites termed MP, A, B, and C and used, here, corresponded to crystallite sizes of about 100, 600, 900, and 1400 Å, respectively. For substituted magnetites, the size was about 600 Å. For each substitution ratio dealt with in this study ( $x = 0$ ,  $x = 0.27$ , and  $x = 0.40$ ) the spinels are inverse and may be formulated as  $\text{Fe}^{3+}[\text{Fe}^{2+}\text{Fe}_{1-x}^{3+}\text{M}_x^{3+}]_2\text{O}_4^{2-}$ , putting into square brackets those ions on octahedral positions. The different  $\alpha$  conversion ratios were obtained in thermobalance by establishing the ratio of weight gain corresponding to the partial oxidation expected to the full oxidation of  $\text{Fe}^{2+}$  ions. The substitution involving only trivalent ions, the number of vacancies due to total oxidation, does not change and can be referred to when calculating the conversion ratio.

For instance, the inverse spinels considered above and partially oxidized may be written as  $\text{Fe}^{3+}[\square_{\delta}\text{Fe}_{1-3\delta}^{2+}\text{Fe}_{(1-x)+2\delta}^{3+}\text{M}_x^{3+}]_2\text{O}_4^{2-}$  with  $\delta = \frac{1}{3}$  when oxidation is total, i.e., when  $\alpha = 1$ . We have also verified, from specific area measurements, that the crystallite size of the partially oxidized materials shows no change with respect to that of initial materials.

### Experimental

Both the ir absorption and the X-ray diffraction techniques have already been described (5, 6) and prove particularly interesting in studying such spinel-type compounds where an order-disorder phenomenon occurs (7, 8), for concerning structure both of them provide different but supplementary information.

The ir absorption measurements were carried out by means of the CsI pellet technique. For this purpose pellets (diameter 1 cm) were pressed to give a mixture of powdered ferrite and CsI in a weight ratio of 5:1000. A 200-mg CsI pellet was used as reference. All these spectra were recorded on an ir 4250 over the range 200–700  $\text{cm}^{-1}$ . Specimens between polythene plates were also examined over the range 40 to 200  $\text{cm}^{-1}$  using a far-ir Fourier spectrophotometer but no further absorption bands could be detected in this region.

X-Ray diffraction patterns were taken using  $\text{CoK}\alpha$  radiation for angles  $\theta$  from 7 to 45°. No trace of hematite was detected in any sample. Although oxidations into lacunar  $\gamma$ -phases occur at relatively low temperatures and pressures (9) (less than 250°C and 12 Torr, respectively, for slightly substituted magnetites), these must still be lowered to obtain a better low-intensity ray resolution in X-ray diffraction. Indeed, as subsequently shown, the longer the reaction, the better resolved the low-intensity rays, which may be explained by a better crystallization of the material and a better homogenization of

vacancy distribution, throughout the grain (10). Thus for each conversion ratio  $\alpha$ , reaction times of 24 hr and more were used, effecting oxidations at temperatures of about 150°C and oxygen pressures of about 1 Torr.

## Infrared and X-Ray Investigations of Magnetite versus Oxidation Extent

### 1 Results

(a) *Infrared spectra.* At room temperature pure magnetite showed two diffuse bands at 575 and 380  $\text{cm}^{-1}$ , specific to an inverse disordered II-III spinel and a continuous absorption due to large electron exchanges occurring between  $\text{Fe}^{2+}$  and  $\text{Fe}^{3+}$  ions, both in equal amounts on octahedral sites. However, operating at lower temperature this exchange was halted and both peaks appeared sharper and better resolved (Fig. 1c). At 460 and 515  $\text{cm}^{-1}$  two shoulders were also observed. Crystallite size had no influence on this spectrum apart from the fact that both shoulders were better resolved for that sample for which the crystallite size was larger.

The ir spectrum of magnetite during oxidation varied differently depending on crystallite size. For samples A, B, and C the spectrum differed slightly from that in Fig. 2 for sample B. From a certain conversion ratio ( $\alpha > 0.76$  or  $\delta >$  about 1/5), it showed a relatively high number of absorption bands over the range 200–700  $\text{cm}^{-1}$ . Four strong bands occurred at 390, 440, 554, and 635  $\text{cm}^{-1}$  and at least 11 lower bands occurred at 220, 260, 311, 326, 365, 421, 474, 580, 596, 691, and 720  $\text{cm}^{-1}$ , respectively. For the totally oxidized sample (MP), the ir spectrum was different from the previous one (Fig. 2) in that all the low bands were absent and only the four stronger bands remained.

(b) *X-Ray diffraction.* X-Ray diffraction patterns for the angular range from 9 to 21° are shown in Fig. 3. For pure magnetite

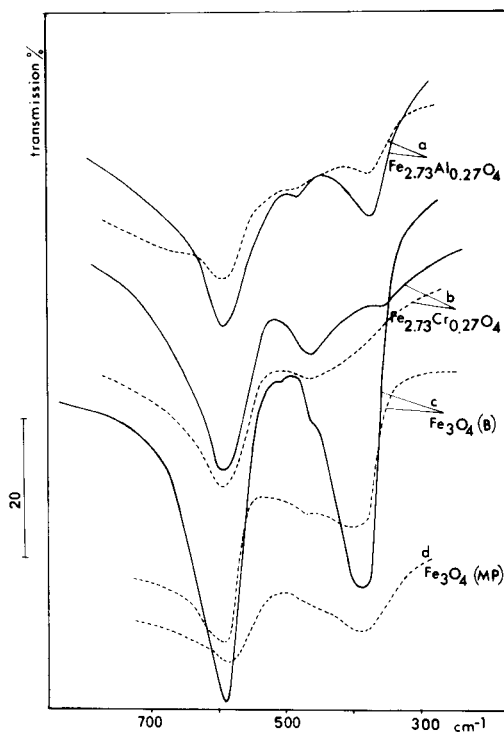


FIG. 1. Infrared spectra of pure magnetites and substituted magnetites. ---, room temperature; —, temperature of 110°K.

samples, they are practically identical and typical of conventional, spinel structure (Figs. 3a and e). A ray broadening is easily observed as crystallite size decreases. X-Ray diagrams of the samples during oxidation show three further rays but these are more numerous for samples A, B, and C as compared with  $\text{Fe}_3\text{O}_4$  (MP) which is totally oxidized (Fig. 3f). It should, however, be noticed that for samples A, B, and C evolution is different depending on the conversion ratio  $\alpha$ . For  $\alpha < 0.45$  the rays are those of pure magnetites while for  $0.45 < \alpha < 0.76$  (Fig. 3b) a few further rays are easily observed, which are those of totally oxidized  $\text{Fe}_3\text{O}_4$  (MP) (Fig. 3f). However, for  $0.76 < \alpha < 1$  (Fig. 3c) the rays are more numerous and correspond to an ordered distribution of vacancies and cations.

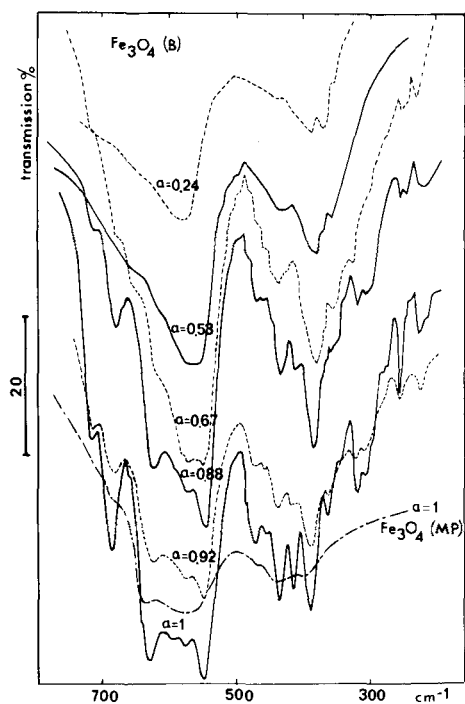


FIG. 2. Infrared spectra of magnetite for different  $\alpha$  conversion ratios.

## 2. Discussion

According to Waldron (11), compounds with  $Fd3m$  spinel structure should possess just four infrared active modes of vibration and therefore exhibit four absorption bands. This has been confirmed experimentally for several normal spinels (5, 12), and for several ferrites (13, 14). However, interactions may always occur between the four ir active modes owing to the fact that they belong to the same representation,  $T_{1u}$  (15). The question becomes still more complex for inverse spinels such as  $Fe_3O_4$  where cations with a different valence are on the same type of site and hence disturb local symmetry. Thus, that atom or those atoms causing a given vibration will be less readily identified. The two strong high-frequency bands  $\nu_1$  and  $\nu_2$  observed in our case at 575 and 380  $cm^{-1}$  may be assigned to the stretching vibrations of the Fe–O bonds. These may be compared

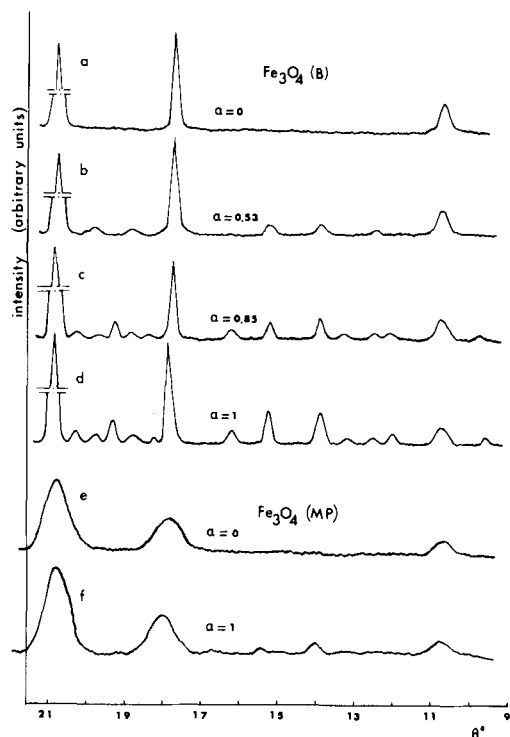


FIG. 3. X-Ray diffraction recordings for  $Fe_3O_4$  samples (B) and (MP) for different  $\alpha$  conversion ratios. Here  $\theta$  is the Bragg angle.

to the peaks found by Waldron (11) at 570 and 380  $cm^{-1}$  and Hafner (16) at 595 and 397  $cm^{-1}$ , respectively.

In the ir absorption spectrum study of solid solutions ( $M, Fe$ ) $_3O_4$ , Ishii *et al.* (17) could calculate the optically active lattice vibrations of  $Fe_3O_4$ . Thus, they could assign the band corresponding to frequency  $\nu_1$  at 565  $cm^{-1}$  to the  $\nu_1(T_{1u})$  mode which is the Fe–O stretching mode of the tetrahedral and octahedral sites and the band corresponding to frequency  $\nu_2$  at 360  $cm^{-1}$  to the  $\nu_2(T_{1u})$  mode which is rather a Fe–O stretching mode of octahedral sites. The bands related to the  $\nu_3(T_{1u})$  and  $\nu_4(T_{1u})$  modes were assigned by these authors to the motion of Fe ions of the tetrahedral sites against those of octahedral sites and an O–Fe–O bending mode of the tetrahedral and octahedral sites, respectively. These bands which may be weak as expected from the calculated vibrational

mode (17) have not been observed down to  $50\text{ cm}^{-1}$  in our experiments. They were, however, mentioned by Grimes and Collett (14) and would be located at 268 and  $178\text{ cm}^{-1}$ , respectively. The two shoulders mentioned at low temperature are attributed to the presence of structural distortions associated with the transformation from cubic to orthorhombic symmetry at  $119^\circ\text{K}$  (18, 19).

For ordered spinel-type compounds White and De Angelis (20) have also determined the number of active modes. This number increases considerably when an order occurs on octahedral or tetrahedral sites. The increase in the number of absorption bands of magnetites A, B, and C during oxidation can thus be interpreted by the occurrence of a certain order in the vacancy and cation distribution on octahedral sites. Indeed for a conversion ratio  $\alpha > 0.76$  the number of absorption bands no longer varies with the oxidation extent and thus the ordering is not affected by the octahedral sites. Of these, the 390-, 440-, 554-, and  $635\text{-cm}^{-1}$  peaks were the most intense and will be assumed to be due to the stretching vibration  $\nu$  of the Fe–O bond. However, for  $\text{Fe}_3\text{O}_4$  (MP), even when totally oxidized, a large number of absorption bands is never observed.

X-Ray diffraction allows us to confirm this order. Although every spinel shows the characteristic lines of the spinel structure for compounds during oxidation we, moreover, observe low-intensity rays of two types:

—Rays forbidden in the space group of conventional spinels but allowed in the case of a cubic cell (belonging to group  $\text{O}^7\text{-P4}_132$ ). These rays occur as soon as a conversion ratio close to  $\alpha = 0.45$  is reached for magnetites A, B, and C and only some of them occur for fully oxidized  $\text{Fe}_3\text{O}_4$  (MP).

—Rays which can only be accounted for by assuming a quadratic cell (ratio  $c/a = 3$ ). They occur only for samples A, B, and C from a conversion ratio  $\alpha = 0.76$ . They show an ordered distribution of cations and

vacancies on octahedral sites. We, indeed, know from magnetic and crystallographic measurements (21) that the vacancies are mainly on octahedral sites.

Infrared and X-ray analysis thus confirm the ordering on octahedral sites. This ordering is possible from a conversion ratio such that  $\alpha = 0.76$  but only for magnetites of size larger than  $600\text{ \AA}$ . Those samples whose size is about  $100\text{ \AA}$  are only partially ordered. This results seems in disagreement with that reported by Hamed and Morrish (2), who found no vacancy ordering on octahedral sites as soon as crystallite size was less than about  $200\text{ \AA}$ .

### **Infrared and X-Ray Investigations of Aluminum or Chromium Slightly Substituted Magnetite versus Its Oxidation Extent**

#### *1. Results*

(a) *Infrared spectra.* For unoxidized samples, as for magnetite, we have only two strong bands (Figs. 1a and b) although the peaks obtained at low temperature are less intense due to substitution which causes the electron exchange on octahedral sites to decrease as shown from electrical conductivity measurements (22). Substitution causes the bands to shift toward high frequencies (5). This slight displacement of the strongest-frequency band is more important for the other band as the frequency rises by more than  $100\text{ cm}^{-1}$  versus frequency  $\nu_2$  of magnetite. For aluminum-substituted magnetite a  $\nu_3$  strong band occurs.

The spectrum evolution during oxidation varies with the substitution ratio but is slightly influenced by the nature of the substituent. For  $x = 0.27$  the spectrum is slightly different from that mentioned for  $\text{Fe}_3\text{O}_4$  (B) oxidation (Figs. 4 and 5). For  $\alpha > 0.80$  we find again the same number of absorption bands. However, for higher substitution ratios ( $x = 0.40$ ) we no longer

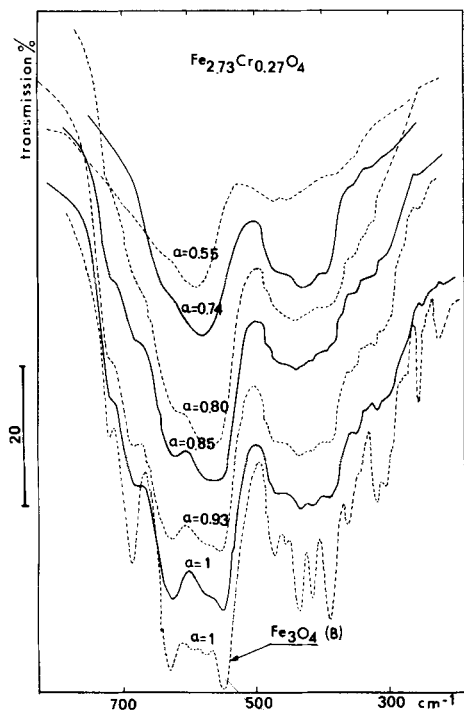


FIG. 4. Infrared spectra of chromium-substituted magnetite ( $x = 0.27$ ) for different  $\alpha$  conversion ratios.

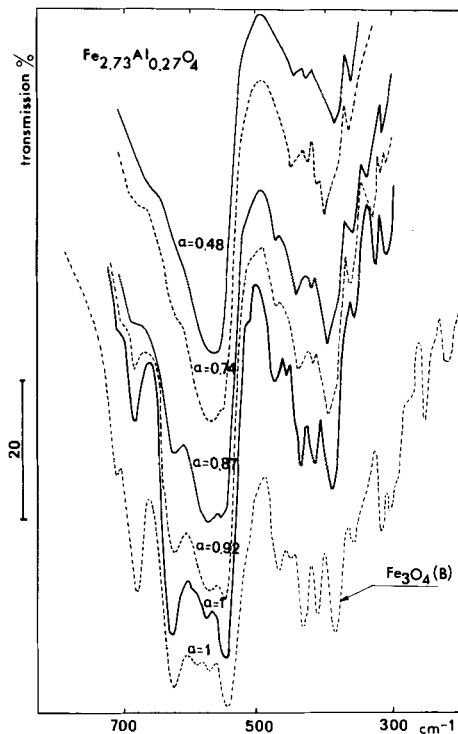


FIG. 5. Infrared spectra of aluminum-substituted magnetite ( $x = 0.27$ ) for different  $\alpha$  conversion ratios.

find a large number of absorption bands even when oxidation is total (Fig. 6). In addition, if both frequency bands around  $554$  and  $635\text{ cm}^{-1}$  are still present for high conversion ratios, the other two strong bands at  $390$  and  $440\text{ cm}^{-1}$  for all  $\gamma$ -phases resulting from magnetite are absent for a composition  $x = 0.40$  along with all the other low-intensity bands. The absence of bands in this region differentiates the spectrum obtained from that of fully oxidized magnetite (MP).

(b) *X-Ray diffraction.* Figure 7 shows that for  $x = 0.27$  the X-ray diagram is little different from that of magnetite (B) during oxidation. The only difference is that the superstructure rays occur for slightly higher conversion ratios and are less intense. For the case of a higher substitution ratio ( $x = 0.40$ ) no further ray is observed during oxidation with respect to the initial spinel.

## 2. Discussion

As in the case of magnetite, the band assignment becomes complex for inverse spinels containing cations not only with different valences but also of different natures, for interactions may always occur among the four ir active modes owing to the fact that they belong to the same representation,  $T_{1u}$  (8). As already discussed in a previous paper (5), the band shift toward high frequencies by introduction of  $\text{Cr}^{3+}$  or  $\text{Al}^{3+}$  ions on octahedral sites agrees with the absorption ranges reported by Preudhomme and Tarte (23) for some condensed octahedral groups.

Concerning the spinel  $x = 0.27$ , during oxidation, the analogy of its ir spectrum with that of magnetite for  $\alpha > 0.80$  leads us to assign the large number of absorption bands to the setting up of an ordering of vacancies and cations on octahedral sites.

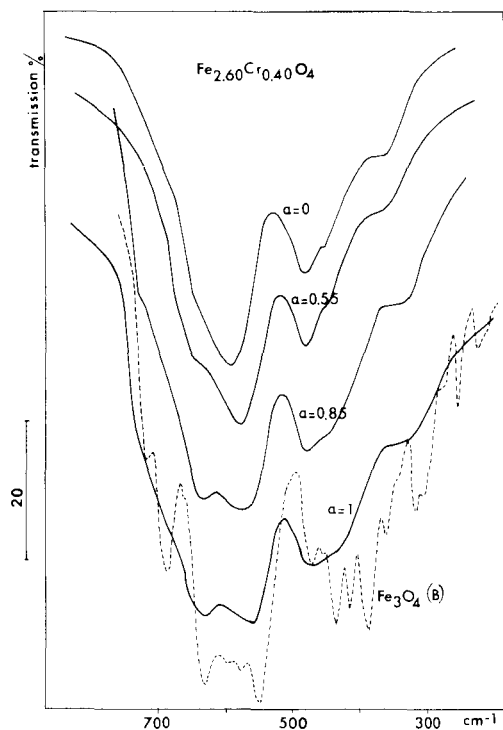


FIG. 6. Infrared spectra of chromium-substituted magnetite ( $x = 0.40$ ) for different  $\alpha$  conversion ratios.

X-Ray analysis confirms this assignment, also by the presence of superstructure rays. However, the small number of absorption bands and the absence of superstructure rays for the spinel  $x = 0.40$ , whatever the conversion rate  $\alpha$ , exclude any ordering on octahedral sites. The same holds true for higher substitution ratios.

### Conclusion

X-Ray and ir investigation allows us to conclude that, from a given conversion ratio ( $\alpha > 0.76$ ), the existence of superstructure rays and a large number of absorption bands for pure or slightly substituted magnetite samples whose crystallite size is above a critical value agrees with a vacancy and cation ordering on octahedral sites. We can state that—following the presence of a relatively low number of absorption bands and the

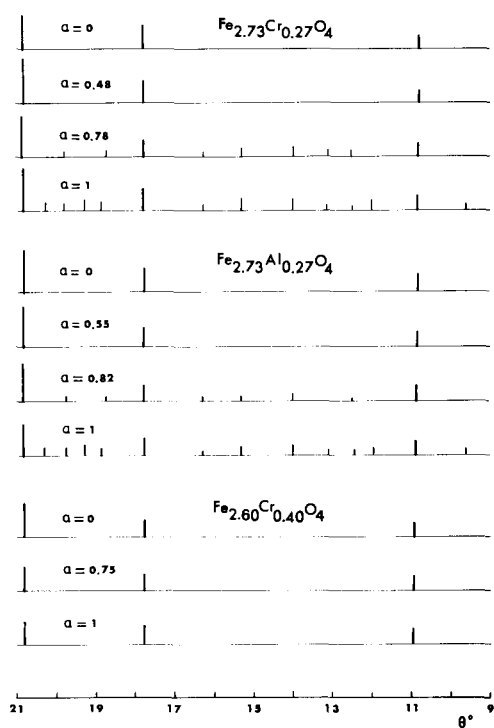


FIG. 7. X-Ray diffraction of substituted magnetite at different compositions. The highest peaks are those of conventional spinel structure.

disappearance of some low-intensity rays—this ordering is only partial for conversion ratios between 0.76 and 0.50 or for fully oxidized magnetites whose crystallite size is about  $100 \text{ \AA}$ . As for magnetites, whose substitution ratio is near or above 0.40 and fully oxidized, the ordering disappears, which is in full agreement with the total absence of superstructure rays in the X-ray diagram and with a large change in the ir spectrum, which shows a relatively limited number of absorption bands over the range  $300\text{--}450 \text{ cm}^{-1}$ . This total absence of ordering does not exclude, however, the fact that all the vacancies are on octahedral sites (3). It has been shown, however, that for very high substitution ratios, i.e., for compounds close to iron(II)aluminate and chromite, the vacancies also occupy tetrahedral sites and this is in the amount of one-third of the

vacancies on tetrahedral sites and two-thirds of those on octahedral sites. These results confirm those of Korobeinikova *et al.* (1), who have also shown that the distribution of these vacancies in the cationic sublattices does not show a preference for a definite type of site, but depends on the chemical and thermal prehistory of the specimen.

## References

1. A. V. KOROBAINIKOVA, V. I. FADEEVA, AND L. A. REZNITSKII, *Zh. Strukt. Khim.* **17**, 860 (1976).
2. K. HAMEDA AND A. H. MORRISH, *Solid State Commun.* **22**, 779 (1977).
3. P. MOLLARD, A. ROUSSET, AND G. DUPRÉ, *Mater. Res. Bull.* **12**, 797 (1977).
4. H. TAKEI AND S. CHIBA, *J. Phys. Soc. Japan* **21**, 1255 (1966).
5. B. GILLOT, F. BOUTON, J. F. FERRIOT, F. CHASSAGNEUX, AND A. ROUSSET, *J. Solid State Chem.* **21**, 375 (1977).
6. B. GILLOT, A. ROUSSET, AND G. DUPRÉ, *J. Solid State Chem.* **25**, 263 (1978).
7. G. BLAISE, *J. Inorg. Nucl. Chem.* **26**, 1473 (1964).
8. J. PREUDHOMME, *Ann. Chim. (Paris)* **9**, 31 (1974).
9. B. GILLOT, *Ann. Chim. (Paris)* **3**, 209 (1978).
10. B. GILLOT, *Mater. Res. Bull.* **13**, 783 (1978).
11. R. D. WALDRON, *Phys. Rev.* **99**, 1727 (1955).
12. K. SIRATORI, A. TSUCHIDA, AND Y. TOMONO, *J. Appl. Phys.* **36**, 1050 (1965).
13. A. MITSUISHI, H. YOSHINAGA, AND S. FUJITA, *J. Phys. Soc. Japan* **13**, 1236 (1958).
14. N. W. GRIMES AND A. J. COLLETT, *Nature Phys. Sci.* **230**, 158 (1971).
15. J. PREUDHOMME, in "Seminaire de Chimie de l'Etat Solide" (J. P. Sichert, Ed.), p. 32, Masson, Paris (1974).
16. S. HAFNER, *Z. Kristallogr.* **115**, 331 (1961).
17. M. ISHII, M. NAKAHIRA, AND T. YAMANAKA, *Solid State Commun.* **11**, 209 (1972).
18. U. BUCHENAU, *Phys. Status Solidi B* **70**, 181 (1975).
19. B. GILLOT, *J. Phys. Chem. Solid* **40**, 261 (1979).
20. W. B. WHITE AND B. A. DE ANGELIS, *Spectrochim. Acta Part A* **23**, 985 (1967).
21. A. ROUSSET, J. PARIS, AND P. MOLLARD, *Ann. Chim. Part A (Paris)* **7**, 119 (1972).
22. B. GILLOT, J. F. FERRIOT, AND A. ROUSSET, *J. Phys. Chem. Solids* **37**, 857 (1976).
23. J. PREUDHOMME AND P. TARTE, *Spectrochim. Acta Part A* **27**, 961 (1971).